EARTHQUAKE ENGINEERING AND STRUCTURAL DYNAMICS
Earthquake Engng Struct. Dyn. 2000; **29**: 823–846

Simplification of strong ground motion considering inelastic responses of structures

Yuki Sakai*,†, Tadao Minami‡ and Toshimi Kabeyasawa‡

Earthquake Research Institute, University of Tokyo, 1-1-1 Yayoi, Bunkyo-ku, Tokyo 113-0032, Japan

SUMMARY

Simplification of strong ground motions to 1 cycle sine waves was investigated from the elastic and inelastic earthquake response analyses and response analyses under sine wave input using single-degree-of-freedom systems. Strong ground motions could be simplified to 1 cycle sine waves if large plastic deformations, with ductility factor more than 2, were assumed. This is because the approximate maximum responses from input sine waves are determined by the initial response cycle, due to period elongation and plastic energy dissipation of the systems. A sine wave whose acceleration amplitude is the peak ground acceleration (PGA) and whose period is that of an equivalent 1 cycle sine wave is proposed. The period of an equivalent sine wave is easily obtained from the elastic response acceleration spectrum of a seismic record. This means that the inelastic responses are approximately determined by the PGA and an equivalent 1 cycle sine wave period. Therefore, an equivalent 1 cycle sine wave period provides a single index to express the frequency characteristics of a strong ground motion.

KEY WORDS: simplification; earthquake strong motion prediction; required strength spectrum; single-degree-of-freedom system; 1 cycle sine wave; ductility factor

1. INTRODUCTION

In earthquake-resistant design of structures, it is essential to adequately predict the input strong ground motion. Accelerograms, however, are very complicated and difficult to predict in detail. Near-field strong ground motions, such as those of the 1994 Northridge and 1995 Hyogoken–Nanbu earthquakes which caused severe damage, are particularly complicated because many factors (e.g., the inhomogeneity on a fault and directivity) must be considered.

Simplification of strong ground motions may make the prediction easier and be useful for designing earthquake-resistant structures. Similarities between response spectra from simple

* Correspondence to: Yuki Sakai, Earthquake Research Institute, University of Tokyo, 1-1-1 Yayoi, Bunkyo-ku, Tokyo 113-0032, Japan
† Research Associate.
‡ Professor.

Received 8 January 1999
Revised 20 November 1999
Accepted 16 December 1999

pulse waves and strong ground motions have been reported [1], but there are no reports on the simplification of strong ground motions considering the detailed inelastic responses of structures, which are essential in earthquake-resistant design.

Here, we propose a method of simplifying strong ground motions to 1 cycle sine waves without changing the inelastic responses of structures.

Elastic and inelastic earthquake response analyses and response analyses under sine wave input were conducted using single-degree-of-freedom systems (SDOF systems) for simplicity.

Analytical procedures:

(1) Inelastic earthquake response analyses were made to calculate the required strength spectra which give maximum response ductility factors within constant values. The close relationship between the spectra and actual damage to structures was shown.
(2) Elastic and inelastic response analyses under sine wave input were made to examine the relationship between the responses and sine wave parameters, e.g. the acceleration amplitude, period and number of cycles.
(3) Inelastic response analyses under the input of 1 cycle sine waves whose acceleration amplitudes are the peak ground accelerations (PGAs) and whose periods are those derived from strong ground motions (e.g. predominant periods) were made in order to calculate the required strength spectra. The spectra obtained using the strong ground motions and the 1 cycle sine waves were then compared.
(4) The 1 cycle sine wave period which makes the discrepancy minimal between the required strength spectra obtained by strong ground motions and 1 cycle sine waves was investigated. Lastly, a method to simplify the strong ground motions to the 1 cycle sine waves was established.

2. STRONG GROUND MOTIONS USED IN THE ANALYSES

Elastic and inelastic earthquake response analyses of SDOF systems were made using the input strong ground motion records shown in Table I. The peak ground velocity (PGV) was calculated using elastic response analyses for a period of 15 s and a damping factor of 0.707, instead of integrating accelerogram data, in order to avoid velocity remaining after the end of earthquake records [2].

The FKI, KBP, and TKT records were taken in or near areas severely damaged by the 1995 Hyogoken–Nanbu earthquake [3, 4]. The PGAs in these records are very high, but there are many records of even higher accelerations which caused less structural damage. KSR, OTB, AKS, PCD, and CYC are records that have very high PGAs, but for which structural damage was not very great because the predominant period was short [5–9]. On the other hand, the PGVs of KSR, OTB, AKS, PCD, and CYC are far smaller than those of FKI, KBP and TKT. The SCT and CDA records are those of the 1985 Michoacan Mexico earthquake which caused severe damage even though their PGAs were small. The PGA alone therefore does not express the actual damage to structures. ELC, TFT, HAC, and THU are records often used in the earthquake-resistant design of important structures.

Although response analyses were made for all the records, only the results of the six representative records are shown in the figures, with the symbol * on the shoulder of the ID in Table I.

Table I. Input strong ground motion records used.

ID	Station	Direction	Earthquake	PGA	PGV
FKI*	Osaka Gas Fukiai Station	NS	1995 Hyogoken–Nanbu	802	130.4
TKT	JR Takatori Railroad Station	NS	1995 Hyogoken–Nanbu	606	124.2
KBM	Kobe Meteorological Agency	NS	1995 Hyogoken–Nanbu	818	85.1
KBP	Kobe Port 8th Bank	NS	1995 Hyogoken–Nanbu	686	176.9
KBU	Kobe University	NS	1995 Hyogoken–Nanbu	270	55.4
SLM*	Sylmar	EW	1994 Northridge	827	125.7
TRZ	Tarzana	EW	1994 Northridge	1745	113.6
NWH	Newhall	EW	1994 Northridge	572	69.4
STM	Santa-Monica	EW	1994 Northridge	866	43.5
KSR*	Kushiro Meteorological Agency	EW	1993 Kushiro-oki	711	33.1
OTB*	Hokkaido Otobe-cho	EW	1993 Hokkaido-Nansei-oki (aftershock)	1568	57.1
PCD	Pacoima Dam	EW	1971 San-Fernando	1055	53.8
CYC	Coyote Lake Dam	EW	1984 Morgan Hill	1138	76.1
AKS	Akkesi	NS	1994 Hokkaido-Toho-oki	1061	50.9
SCT*	SCT1	EW	1985 Michoacan Mexico	168	60.9
CDA	CDAF	EW	1985 Michoacan Mexico	95	37.8
ELC*	El-Centro	NS	1940 Imperial Valley	342	34.8
TFT	Taft	EW	1952 Arvin-Tahachapi	176	17.7
HAC	Hachinohe Port	EW	1968 Tokachi-oki	182	33.9
THU	Tohoku University	NS	1978 Miyagiken-oki	238	41.0

PGA: peak ground acceleration (cm/sec.^{2}), PGV: peak ground velocity (cm/sec.).

Time histories of ground acceleration for the six records are shown in Figure 1. FKI and SLM are representative of the 1995 Hyogoken–Nanbu and 1994 Northridge earthquakes [10], respectively. Of the 1994 Northridge earthquake records, SLM had the most destructive power [11]. Both FKI and SLM are near-field records with high accelerations and long-period pulses. KSR and OTB are representative of records that have very high PGAs, but for which structural damage was not very great because of the short predominant period [5, 6]. The PGA of OTB is very high but high acceleration occurred only a few times. In contrast, high acceleration occurred many times in the KSR record. SCT is a representative record of the 1985 Michoacan Mexico earthquake which caused severe damage due to its long predominant period and many cyclic reversals. ELC is representative of records often used in designing important earthquake-resistant structures.

Elastic response acceleration spectra with damping factor of 0.05 are shown in Figure 2 for all six records. FKI has a long predominant period and high acceleration responses in the period range longer than 1.0 s; whereas, in the period range shorter than 0.5 s, the response accelerations of KSR and OTB are larger. As this does not correspond to the observed actual damage to structures, the elastic responses do not express damage.

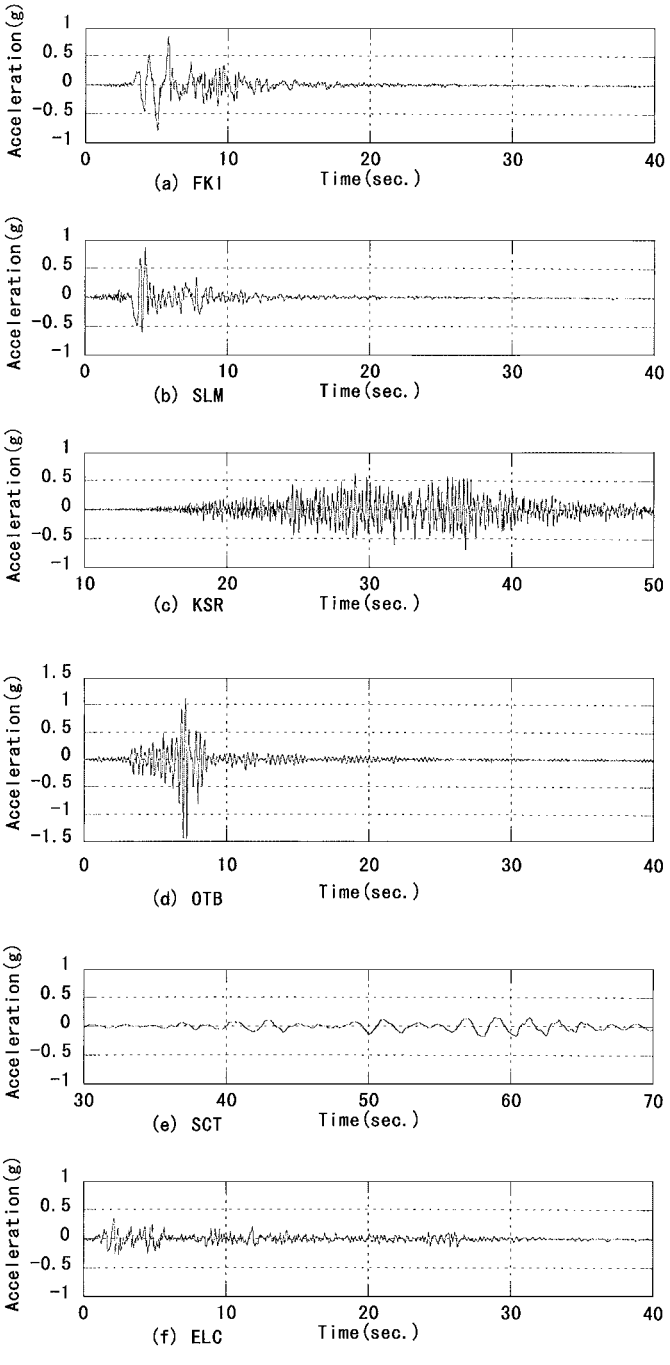

Figure 1. Time histories of ground acceleration.

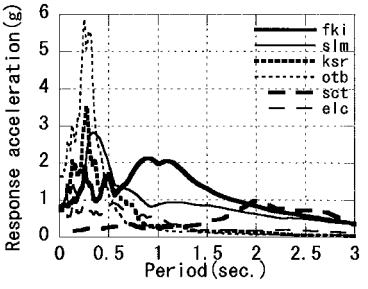

Figure 2. Elastic response acceleration spectra for a damping factor of 0.05.

3. REQUIRED STRENGTH SPECTRA CALCULATED BY INELASTIC EARTHQUAKE RESPONSE ANALYSES

Inelastic earthquake response analyses were made using SDOF systems. Required base shear coefficients which produce constant maximum response ductility factors (called 'allowable ductility factors μ_a') were calculated. Allowable ductility factors μ_a were set at 2, 4 and 8. The required base shear coefficients are calculated instead of the response ductility factors because what we need in earthquake-resistant design is a base shear coefficient to bring the ductility factor within specified values.

The bilinear and bilinear Takeda [12] hysteresis models were used to represent three different energy dissipation capacities. The bilinear Takeda model was used instead of the original Takeda model [13] in order to investigate only the influences of energy dissipation difference. Primary curves of the bilinear Takeda and Takeda models are shown in Figure 3. The ratio of post-yielding stiffness to initial elastic stiffness β was assumed to be 0.01. Unloading stiffness degradation factor α were set at 0 and 0.5 for the bilinear Takeda model. Equivalent viscous damping factors at steady-state resonance for the three energy dissipation capacities are calculated by Equations (1) and (2) [12], and shown in Table II.

$$h_{eq} = \frac{2(1-\beta)^2(\mu-1)}{\pi\mu(1-\beta+\mu\beta)(1-\beta)} \quad \text{for bilinear model} \tag{1}$$

$$h_{eq} = \frac{1}{\pi}\left(1 - \frac{\mu^{\alpha}(1-\beta+\mu\beta)}{\mu}\right) \quad \text{for bilinear Takeda model} \tag{2}$$

where h_{eq} is the equivalent viscous damping factor at steady-state resonance, μ_a the allowable ductility factor and α the unloading stiffness degradation factor.

Figure 4 shows the time histories of the base shear coefficients vs ductility factor responses for these models when the yielding base shear coefficient is 0.3 and the input record is ELC. The elastic periods of systems T were changed from 0.1 to 3.0 s as given in Equation (3). The number of systems becomes 3 energy dissipation capacities $\times$ 3 allowable ductility factor $\times$ 30 periods of

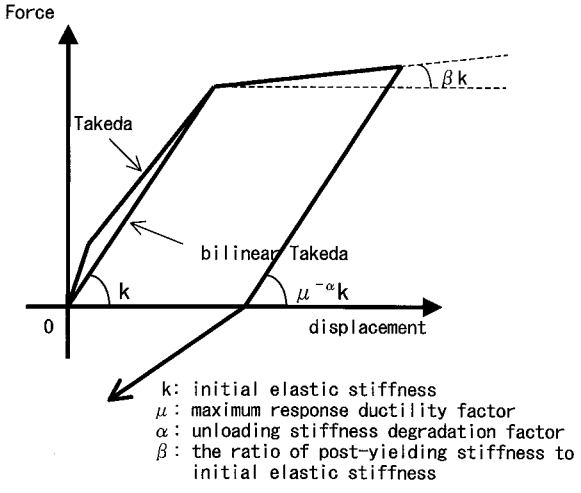

Figure 3. Primary curves of Takeda and bilinear Takeda model.

Table II. Equivalent viscous damping factors at steady-state resonance.

	Allowable ductility factor		
Hysteresis model	2	4	8
Bilinear	0.312	0.459	0.515
Bilinear Takeda ($\alpha = 0.0$)	0.158	0.236	0.276
Bilinear Takeda ($\alpha = 0.5$)	0.091	0.154	0.198

the system = 270.

$$T = 0.1 \times 1.12^N \ (N = 1, 2, \ldots, 30) \ (\text{s}) \tag{3}$$

The required base shear coefficient spectra that give a ductility factor within 2, 4 and 8 (hereafter called 'required strength spectra') are calculated, and shown in Figure 5 for the six representative records. The damping coefficient is assumed to be proportional to instantaneous stiffness with an initial elastic damping factor of 0.05. Although the spectra in Figure 5 are similar, the required base shear coefficients are larger for smaller μ_a and energy dissipation capacities. Compared to the elastic response acceleration spectra in Figure 2, the vertical axis values tend to be smaller because plastic energy dissipation was considered, and the predominant period moved to the short-period region due to period elongation caused by plastic deformation. The predominant period of the FKI record (about 1.0 s) in Figure 2 therefore shifted to the short-period range, to which most buildings belong [14, 15]. In contrast, the peaks of KSR and OTB which, in

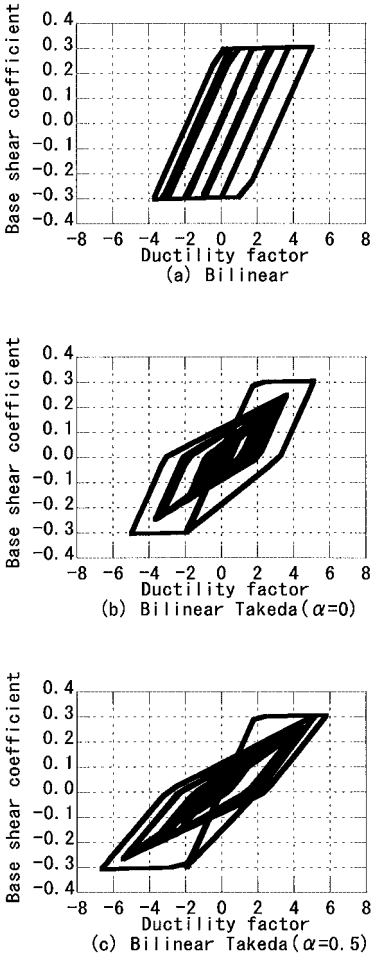

Figure 4. Time histories of base shear coefficients vs the ductility factor response for the three energy dissipation capacities.

Figure 2, have very high elastic response acceleration in the short-period range shifted to even shorter period range of less than 0.3 s, to which few buildings belong [14, 15]. Consequently, FKI require much greater strength than KSR and OTB in the period range longer than 0.3 s, although KSR has almost the same PGA as FKI, and OTB has a much higher PGA. These results correspond to the actual damage to structures. We therefore adopted the required strength spectra as the inelastic response spectra in our simplification of strong ground motions to 1 cycle sine waves.

On the basis of the required strength spectra, large strength is required in the case of strong ground motions with a predominant period longer than that of the system due to the plastic elongation of the systems. The frequency characteristics of strong ground motions as well as the PGA therefore must be considered when evaluating the required strength spectra.

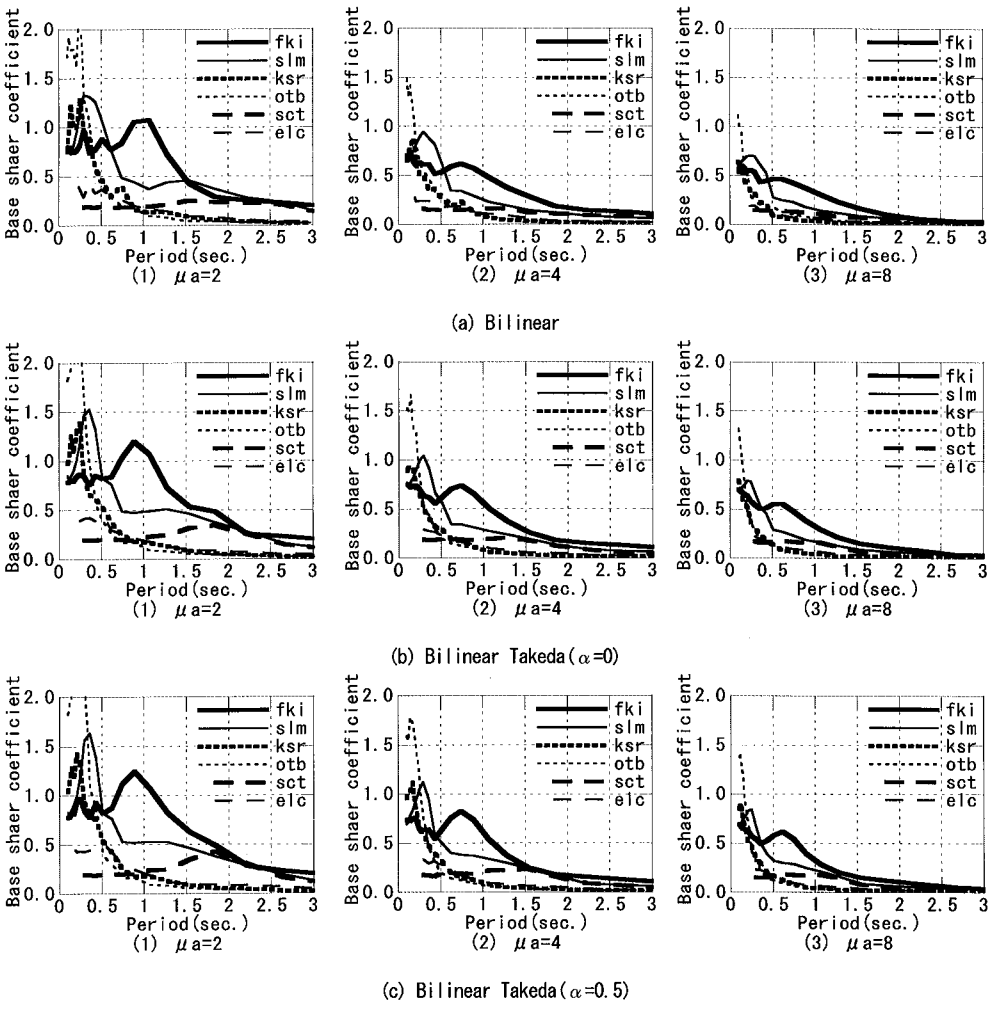

Figure 5. Required strength spectra.

4. ELASTIC AND INELASTIC RESPONSE ANALYSES TO SINE WAVE INPUT

The above findings show that the frequency characteristics, in addition to the PGA, is a major factor for evaluating inelastic seismic responses. Elastic and inelastic response analyses therefore were made with SDOF systems under sine wave input expressed by the PGA, frequency and number of cycles. Parameters of the input sine waves are the acceleration amplitude (0.25, 0.5, 1.0 and 2.0 g), period (0.25, 0.5, 1.0 and 2.0 s), and number of cycles (1, 2, 4 and 8). Examples of the elastic response acceleration spectra with the damping factor of 0.05 are shown in Figure 6.

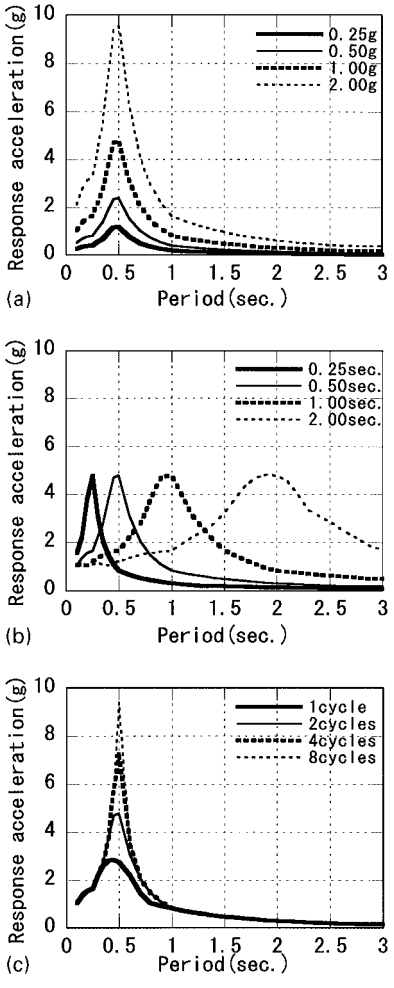

Figure 6. Elastic response acceleration spectra for 0.05 damping under sine wave input: (a) parameter: acceleration amplitude (for 0.5 s period and 2 cycles); (b) parameter: period (for 1g amplitude and 2 cycles); (c) parameter: number of cycles (for 1g amplitude and 0.5 s period).

4.1. Results of elastic response analyses

Response acceleration spectra for the four different acceleration amplitudes of input sine waves are shown in Figure 6(a), when period and number of cycles are 0.5 s and 2, respectively. Response acceleration is linearly related to the PGA with similar results for other periods and numbers of cycles.

The spectra for the four different periods of sine waves are shown in Figure 6(b) when acceleration amplitude and number of cycles are 1 g and 2, respectively. The spectra shifted along the horizontal axis according to the sine wave period. Similar results were obtained for other acceleration amplitudes and numbers of cycles.

The spectra for the four different numbers of cycles of sine waves are shown in Figure 6(c) when acceleration amplitude and period are $1g$ and 0.5 s, respectively. The response acceleration is magnified as the number of cycles increase because of the resonance phenomenon. Similar results were obtained for other acceleration amplitudes and periods. These results for the elastic response analyses were as expected.

4.2. Results of inelastic response analyses

Required strength spectra were calculated in the same way as in the inelastic earthquake response analyses with examples shown in Figures 7–9. Parameters of the systems are the same as those in

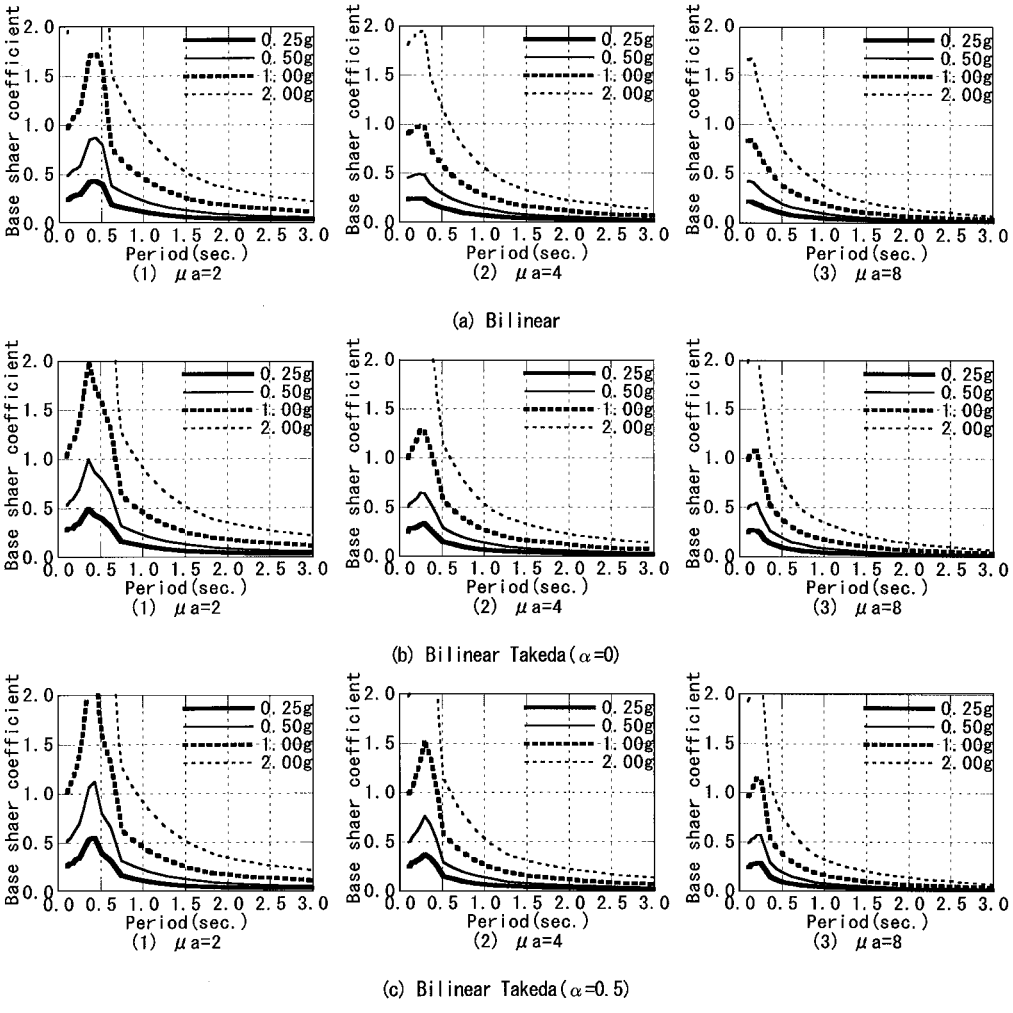

Figure 7. Required strength spectra for four acceleration amplitudes of sine waves (for 0.5 s period and 2 cycles).

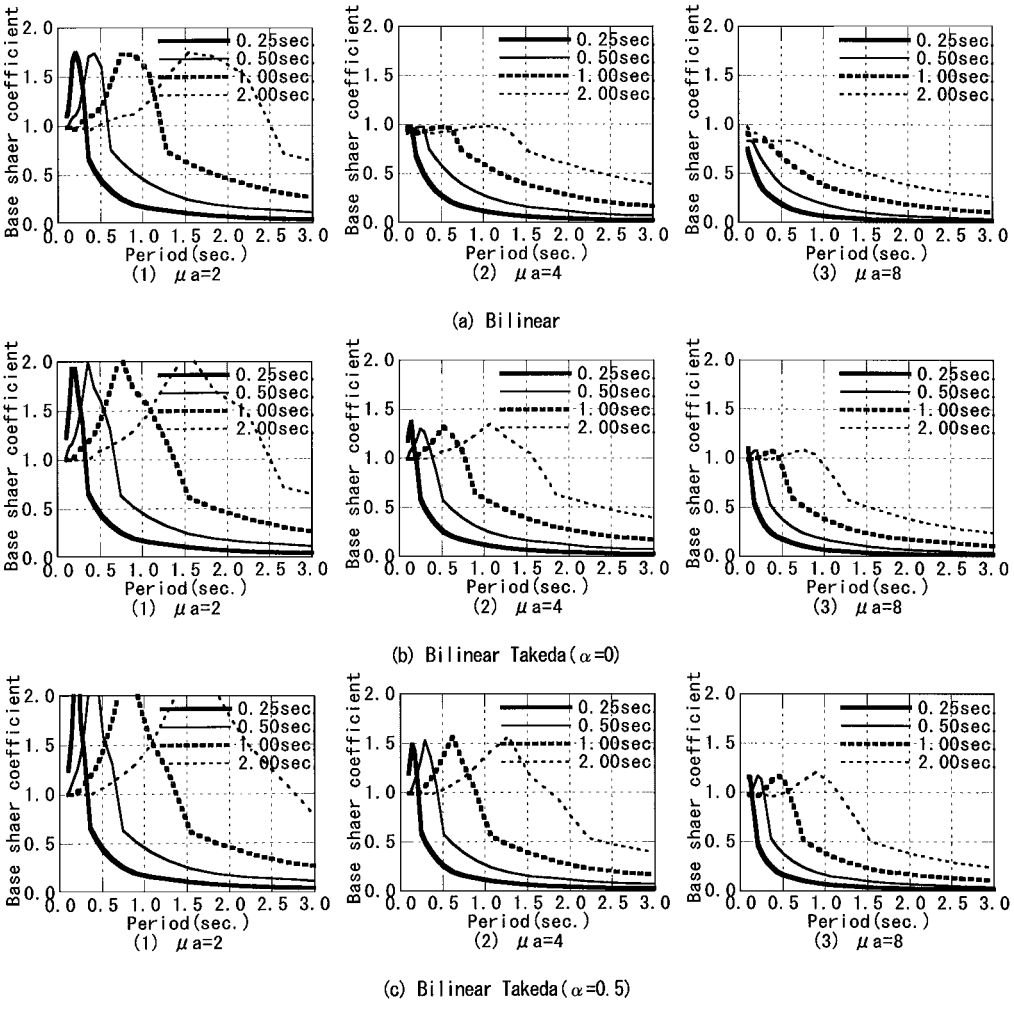

Figure 8. Required strength spectra for four periods of sine waves (for 1g amplitude and 2 cycles).

the earthquake response analyses, i.e. the energy dissipation capacities through the hysteresis model (the bilinear and bilinear Takeda model ($\alpha = 0$ and 0.5)) and the allowable ductility factors μ_a (2, 4 and 8).

The spectra for the four acceleration amplitudes of input sine waves are shown in Figure 7 for a 0.5 s period and 2 cycle sine wave. They are linearly related to the PGA as in the elastic spectra shown in Figure 6(a). They are larger for smaller allowable ductility factor μ_a and energy dissipation capacities. This is similar to the earthquake response analyses findings in Figure 5. Compared to the elastic spectra in Figure 6(a), the vertical axis values tend to be smaller because of plastic energy dissipation, and the predominant period shifted to the short-period region

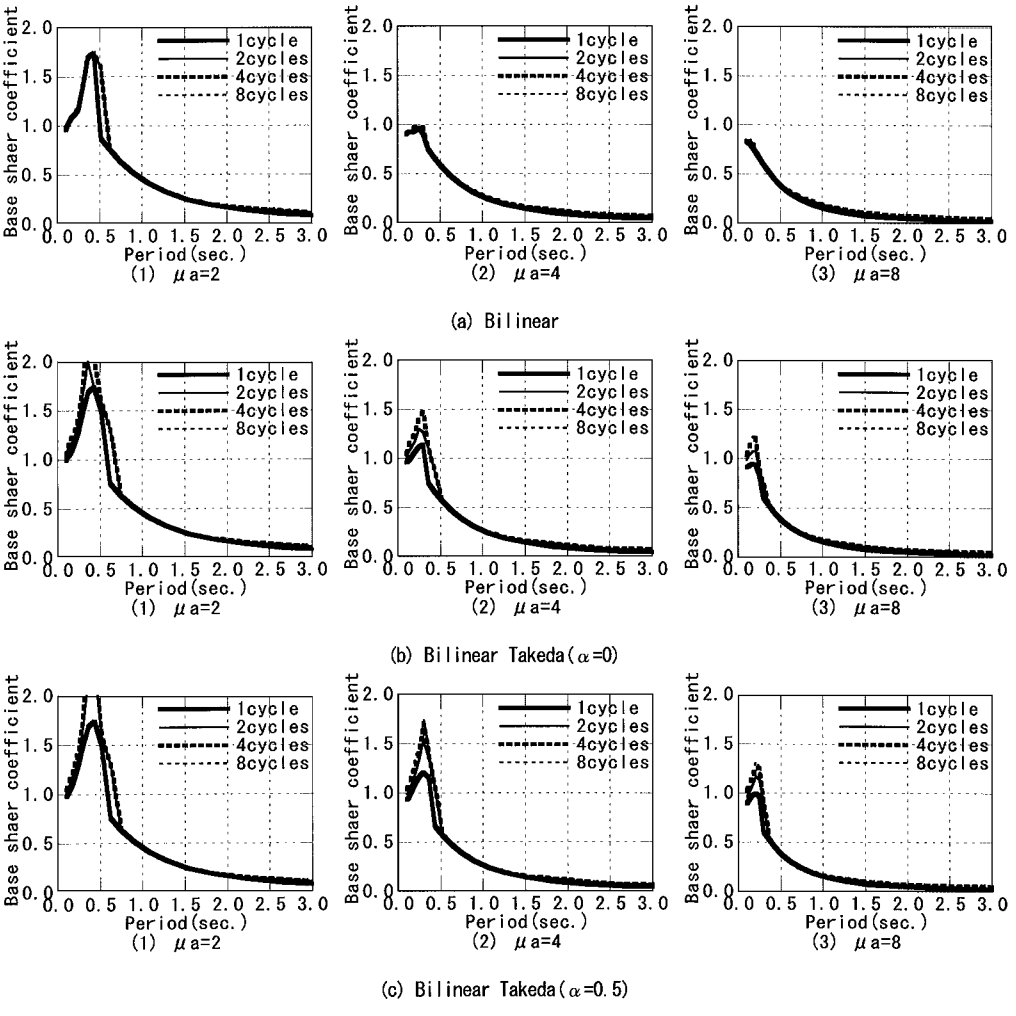

Figure 9. Required strength spectra for four cycles of sine waves (for $1g$ amplitude and 0.5 s period).

because of period elongation caused by plastic deformation, similar to the required strength spectra in Figure 5. Similar results were obtained for other periods and numbers of cycles.

The spectra for the four different periods of input sine waves are shown in Figure 8 for a $1g$ amplitude and 2 cycle sine wave. Compared to the elastic systems in Figure 6(b), the peaks of the spectra shifted to the short-period region due to the period elongation caused by plastic deformation. Therefore, in the longer than 0.3 s-period region of most buildings [14, 15], the required strength spectra are greater for longer sine wave periods when the allowable ductility factor μ_a is larger than 2 or the input sine wave period is shorter than 1.0 s. Similar results were obtained for other acceleration amplitudes and numbers of cycles.

When the parameter is the number of cycles of the input sine wave, the results differ markedly from those of the elastic response analyses. The spectra for the four different numbers of cycles of input sine waves are shown in Figure 9 for a 1g amplitude and 0.5 s period.

The effect of resonance phenomenon, exhibited by the elastic systems, is very small in the inelastic systems; as a whole, the required strength spectrum is not magnified with the larger number of cycles. This trend is more clearly observed in the high-energy dissipation capacity hysteresis model or for large allowable ductility factor; i.e. when the equivalent viscous damping factors in Table II are large. This is because the resonance phenomenon did not occur due to period elongation of the systems, and responses are quickly attenuated by large equivalent viscous damping from plastic energy dissipation. Time histories of the response ductility factor and those of the base shear coefficient vs ductility factor response under 8 cycles of sine waves are shown in Figures 10 and 11, respectively. The responses quickly reached the steady state after the first cycle. For the longer-period systems in particular, displacement shifts by free vibration occurred only in the beginning, with displacement after the first cycle not exceeding the first peak. Similar results were obtained for other acceleration amplitudes and periods. This means that when large plastic deformation is expected, as in the case of an allowable ductility factor larger than 2, the number of cycles of sine waves becomes irrelevant to the maximum response, and only the acceleration amplitude and period need to be considered when evaluating the required strength spectrum.

5. COMPARISON OF REQUIRED STRENGTH SPECTRA FROM STRONG GROUND MOTIONS AND 1 CYCLE SINE WAVES

The required strength spectra under sine wave input were shown to be approximately determined by the first cycle. Here, the required strength spectra from 1 cycle sine waves are calculated and

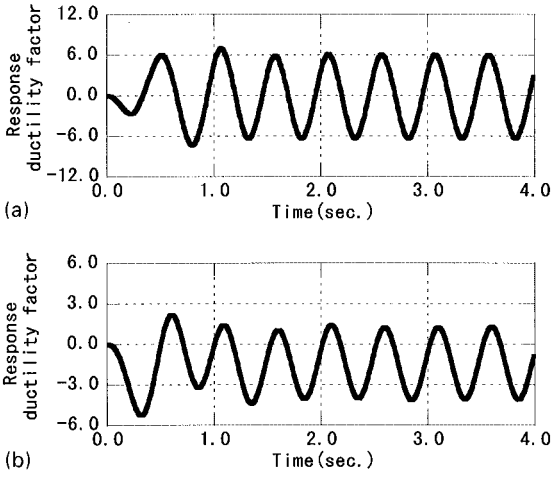

Figure 10. Time histories of response displacement under an 8 cycle sine wave input with 1g amplitude and 0.5 s period (hysteresis model: bilinear Takeda ($\alpha = 0$)); (a) period: 0.25 s, yielding base shear coefficient: 1.0; (b) period: 0.50 s, yielding base shear coefficient: 0.5.

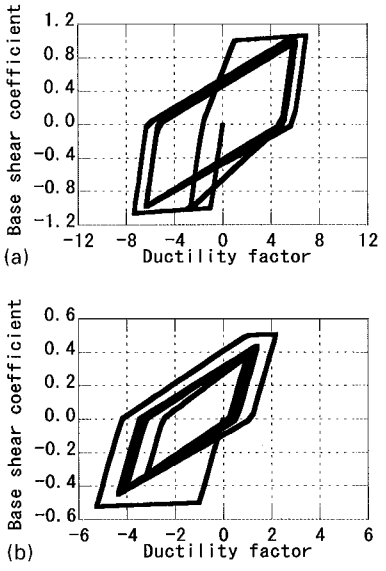

Figure 11. Time histories of the base shear coefficient vs the ductility factor response under an 8 cycle sine wave input with 1g amplitude and 0.5 s period (hysteresis model: bilinear Takeda ($\alpha = 0$)): (a) period: 0.25 s, yielding base shear coefficient: 1.0; (b) period: 0.50 s, yielding base shear coefficient: 0.5.

compared with the spectra from strong ground motions. The amplitude of the 1 cycle sine waves is assumed to be equal to the PGA while three kinds of periods were considered:

(1) predominant period in the elastic response acceleration spectra (Figure 2) (T_p);
(2) mean period [16] defined in Equation (4) (T_m)

$$T_m = \frac{\sum_i C_i^2 (1/f_i)}{\sum_i C_i^2} \quad \text{for } 0.25 \text{ Hz} \leqslant f_i \leqslant 20 \text{ Hz}, \tag{4}$$

where C_i is the Fourier amplitude of the entire accelerogram, and f_i the discrete Fourier transform frequencies between 0.25 and 20 Hz.

(3) period calculated from the PGA and PGV in Equation (5) (T_v)

$$T_v = \frac{2\pi V_{max}}{A_{max}} \tag{5}$$

where A_{max} is the PGA (cm/s^2), and V_{max} the PGV (cm/s).

These periods calculated for each strong ground motion are shown in Table III, while T_e in the table, the period of an equivalent 1 cycle sine wave, is explained in the next section. These periods

Table III. Adopted periods of 1 cycle sine waves (s).

ID	T_p	T_m	T_v	T_e
FKI*	0.90	0.60	1.02	0.96
TKT	1.23	1.10	1.29	1.00
KBM	0.35	0.60	0.65	0.58
KBP	1.50	0.86	1.62	1.55
KBU	1.22	0.92	1.29	1.00
SLM*	0.35	0.55	0.96	0.54
TRZ	0.33	0.27	0.41	0.36
NWH	0.32	0.39	0.76	0.66
STM	0.22	0.31	0.32	0.27
KSR*	0.27	0.27	0.29	0.30
OTB*	0.25	0.17	0.23	0.17
PCD	0.42	0.23	0.32	0.39
CYC	0.25	0.40	0.42	0.33
AKS	0.18	0.12	0.30	0.18
SCT*	2.03	1.17	2.28	2.00
CDA	2.92	1.78	2.50	2.60
ELC*	0.25	0.39	0.64	0.66
TFT	0.44	0.36	0.63	0.56
HAC	0.35	0.68	1.17	1.00
THU	0.96	0.43	1.08	0.81

are the expected values based on the frequency characteristics of the records. They are short for the short-period-dominated records KSR, OTB, PCD, CYC, and AKS, and long for the long-period-dominated records SCT and CDA. They have scattered values, however, for SLM, ELC, and HAC.

Response analyses were made using these three periods for the 1 cycle sine wave input and the required strength spectra were then calculated.

Spectra from 1 cycle sine waves with period T_p, are shown in Figure 12 for the six representative records. Although Figures 12 and 5 are similar on the whole, even in the case of KSR and SCT which have numerous cyclic reversals, the spectra for OTB significantly differ. For example, the required base shear coefficient for the bilinear Takeda model ($\alpha = 0$, $\mu_a = 4$) for the 0.5 s period system in Figure 12(b) (2) is about twice the value shown in Figure 5(b)(2).

The discrepancy between the required strength spectra from strong ground motions and 1 cycle sine waves was measured by the difference ratio defined in Equation (6).

$$D_P(P, R, H, \mu_a, T) = \frac{|S(R, H, \mu_a, T) - S_1(P, R, H, \mu_a, T)|}{S(R, H, \mu_a, T)} \tag{6}$$

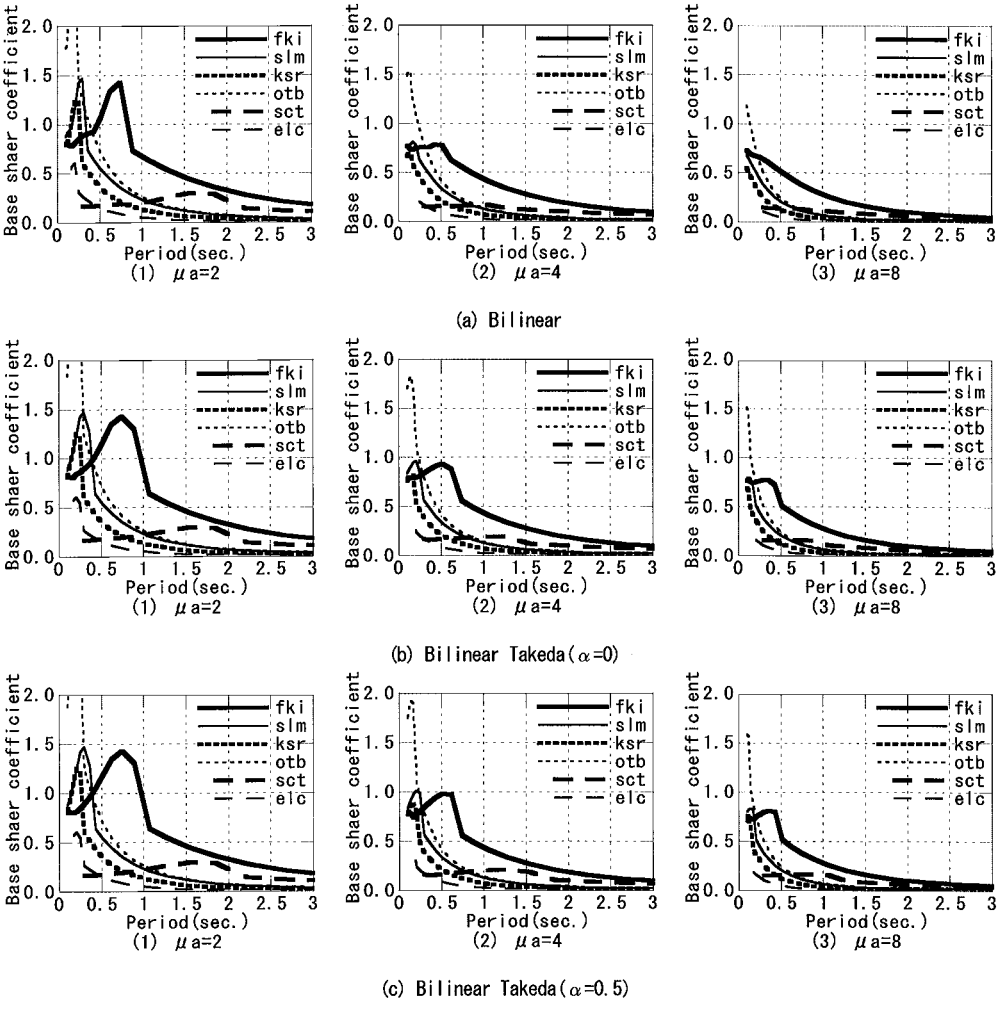

Figure 12. Required strength spectra from 1 cycle sine waves with the predominant periods.

where P is the period of the sine wave (T_p, T_m, T_v); R the records (20 records in Table I); H the hysteresis model (bilinear, bilinear Takeda ($\alpha = 0, 0.5$)); μ_a the allowable ductility factor (2, 4, 8); T the elastic period of the system given in Equation (3); $S(R, H, \mu_a, T)$ the required base shear coefficient from a strong ground motion for each R (corresponding record), H, μ_a, and T; and $S_1(P, R, H, \mu_a, T)$ the required base shear coefficient from a 1 cycle sine wave for each P, R, H, μ_a, and T.

The averages of the difference ratios of all (three hysteresis models $H \times 3$ allowable ductility factors $\mu_a \times 30$ elastic periods for the system T) systems $\bar{D}_P(P, R)$ for each period of a 1 cycle sine wave, P, and each record, R, obtained by Equation (7) are shown in Table IV. The average of the

Table IV. Averages of the difference ratios in all systems $\bar{D}_{\mathrm{P}}(P, R)$ and difference ratios in all systems and records $\bar{\bar{D}}_{\mathrm{P}}(P)$.

ID	T_{p}	T_{m}	T_{v}	T_{e}
FKI*	0.15	0.26	0.16	0.15
TKT	0.22	0.18	0.24	0.17
KBM	0.28	0.21	0.19	0.10
KBP	0.09	0.13	0.11	0.11
KBU	0.13	0.20	0.14	0.19
SLM*	0.32	0.14	0.38	0.14
TRZ	0.17	0.22	0.28	0.20
NWH	0.33	0.27	0.25	0.15
STM	0.24	0.26	0.27	0.23
KSR*	0.12	0.12	0.10	0.10
OTB*	0.44	0.16	0.36	0.16
PCD	0.25	0.28	0.16	0.20
CYC	0.29	0.27	0.22	
AKS	0.21	0.32	0.71	0.21
SCT*	0.11	0.18	0.11	0.10
CDA	0.08	0.09	0.07	0.07
ELC*	0.34	0.23	0.13	0.15
TFT	0.11	0.17	0.12	0.08
HAC	0.32	0.17	0.18	0.12
THU	0.15	0.27	0.20	0.10
AVE	0.22	0.21	0.23	0.15

difference ratios of all 20 records for each period, $\bar{\bar{D}}_{\mathrm{P}}(P)$, obtained by Equation (8) is

$$\bar{D}_{\mathrm{P}}(P, R) = \frac{1}{3}\frac{1}{3}\frac{1}{30}\sum_{H}\sum_{\mu_{\mathrm{a}}}\sum_{T} D_{\mathrm{P}}(P, R, H, \mu_{\mathrm{a}}, T) \tag{7}$$

$$\bar{\bar{D}}(P) = \frac{1}{20}\frac{1}{3}\frac{1}{30}\sum_{R}\sum_{H}\sum_{\mu_{\mathrm{a}}}\sum_{T} D_{\mathrm{P}}(P, R, H, \mu_{\mathrm{a}}, T) \tag{8}$$

where $D_{\mathrm{P}}(P, R, H, \mu_{\mathrm{a}}, T)$ is the difference ratio between the required base shear coefficient from a strong ground motion and a 1 cycle sine wave, as given in Equation (6).

The average value of all the systems and all the records, $\bar{\bar{D}}_{\mathrm{P}}(P)$, is about 0.2. The required strength therefore can be evaluated using 1 cycle sine waves with about 20 per cent discrepancy. For some records, however, the average values of all systems $\bar{D}_{\mathrm{P}}(P, R)$ are greater than 0.3 (underlined in Table IV) showing that there is a large discrepancy between Figures 5 and 12.

For T_{p}, T_{m}, and T_{v}, the averages of the difference ratios of all systems and records $\bar{\bar{D}}_{\mathrm{P}}(P)$ are almost the same, but there are fewer cases of high $\bar{D}_{\mathrm{P}}(P, R)$ for T_{m} than for T_{p} and T_{v}.

Figure 13 shows the difference ratios $D_P(P, R, H, \mu_a, T)$ for the six representative records when the hysteresis model is bilinear Takeda ($\alpha = 0$) and the allowable ductility factor μ_a is 4. The difference ratios $D_P(P, R, H, \mu_a, T)$ vary with the record, with very high values for certain records; record OTB for T_p and SLM and OTB for T_v. There are, however, no such cases for the mean period T_m. A similar tendency was seen with other hysteresis models and allowable ductility factor μ_a .Of the three periods, the mean period T_m therefore is the most suitable for 1 cycle sine waves.

6. METHOD OF CALCULATING THE EQUIVALENT PERIOD OF 1 CYCLE SINE WAVES

Earlier we showed that the required strength spectra could be evaluated by 1 cycle sine waves with a 20 per cent average discrepancy, but except for the mean period, T_m, the discrepancy was high for particular cases. Here we calculate periods of 1 cycle sine waves using elastic response acceleration spectra in order to lessen the discrepancy. The acceleration amplitude of the 1 cycle sine wave is assumed to be equal to the PGA.

The period of a 1 cycle sine wave was calculated in order to minimize the discrepancy between the elastic response acceleration spectra from a strong ground motion and a 1 cycle sine wave. Elastic response acceleration spectra instead of required strength spectra were used because they could be calculated more easily and required strength spectra varies with hysteresis models and allowable ductility factors of the systems.

The period is calculated by the following method (Figure 14):

(1) The elastic response acceleration spectrum of a 1 cycle sine wave with $1g$ amplitude and 1 s period is calculated for damping factor of 0.05 ($h = 0.05$).
(2) For each record, the spectra obtained in (1) is magnified or reduced in the vertical direction by the ratio of the PGA to $1g$. The acceleration amplitude then becomes the PGA.
(3) For each record, the magnified or reduced spectrum in (2) is magnified or reduced in the horizontal direction ranging from 0.1 to 3.0, corresponding to the periods of 1 cycle sine waves (period magnification factor).
(4) The average of the difference ratios for all the elastic periods defined in Equation (3) between the elastic response acceleration from strong ground motions and 1 cycle sine waves, given in Equation (10), is calculated for each record and each period magnification factor, and the relationship is shown in Figure 15. The factor minimizing the difference ratio average is the period with minimum difference between the elastic response acceleration-spectra from strong ground motions and 1 cycle sine waves.

$$D_E(R, F, T) = \frac{|E(R, T) - E_1(F, T)|}{E(R, T)} \tag{9}$$

$$\bar{D}_E(R, F) = \frac{1}{30} \sum_T D_E(R, F, T) \tag{10}$$

where R is the record; F the period magnification factor which corresponds to the 1 cycle sine wave period; T the elastic period of the system given in Equation (3); $E(R,T)$ the elastic

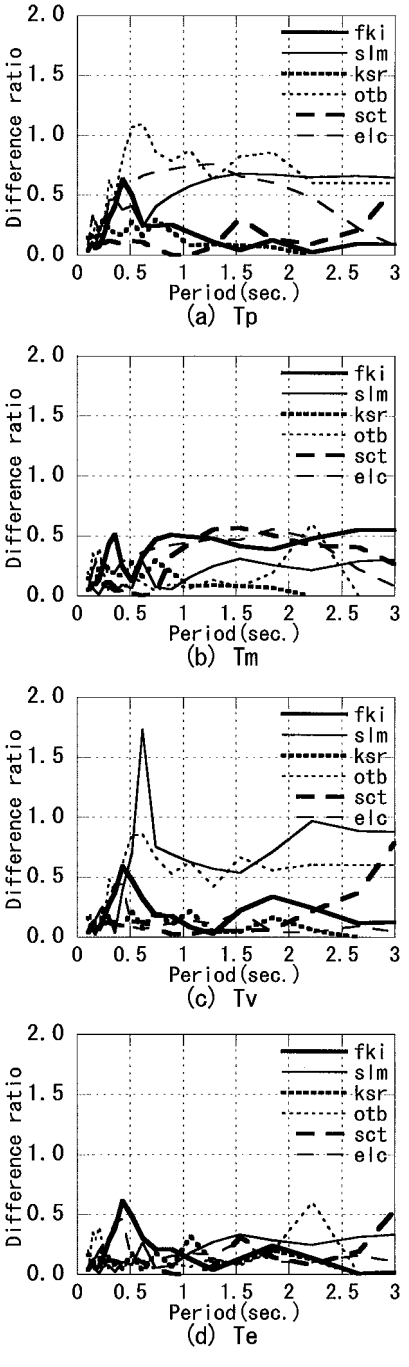

Figure 13. Difference ratios for bilinear Takeda model ($\alpha = 0$) and allowable ductility factor of 4: (a) period of sine wave: T_p; (b) period of sine wave: T_m; (c) period of sine wave: T_v; (d) period of sine wave: T_e.

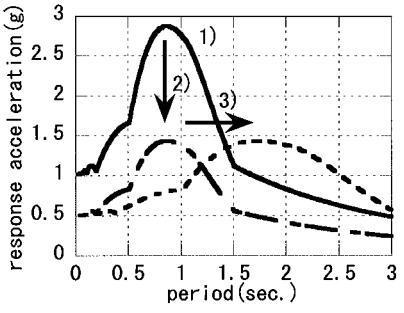

Figure 14. Magnification and reduction of the elastic response acceleration spectra of a 1 cycle sine wave with $1g$ amplitude and 1 s period.

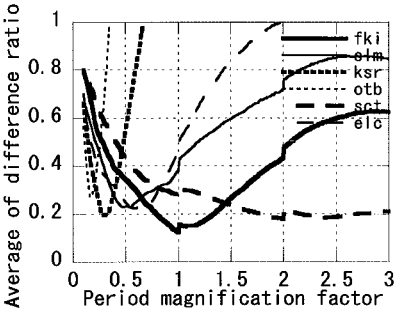

Figure 15. Relationship between the average of the difference ratios and period magnification factors.

response acceleration ($h = 0.05$) from strong ground motion (Figure 2) for each R and T; $E_1(F, T)$ the elastic response acceleration ($h = 0.05$) from a 1 cycle sine wave for each F and T; $D_E(R, F, T)$ the difference ratio between the elastic response acceleration by strong ground motions and 1 cycle sine waves for each R, F and T; and $\bar{D}_E(R, F)$ the average of the difference ratios of all the elastic periods of system T between the elastic response accelerations for each R and F.

The sine wave, whose period is calculated by this method and whose acceleration amplitude is the PGA, can be regarded as equivalent to the original strong ground motion because their elastic response acceleration spectra ($h = 0.05$) are similar. The period calculated by this method therefore is designated 'the equivalent 1 cycle sine wave period T_e'.

Elastic response acceleration spectra ($h = 0.05$) of 1 cycle sine waves having PGA amplitudes and equivalent 1 cycle sine wave periods are shown in Figure 16. They are similar to those in Figure 2.

The equivalent 1 cycle sine wave periods, T_e, shown in Table III, tend to be similar to those of T_m, T_v, and T_p, but differ for individual records.

Next, the required strength spectra of equivalent 1 cycle sine waves were calculated.

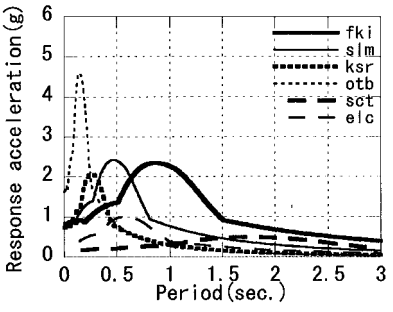

Figure 16. Elastic response acceleration spectra ($h = 0.05$) from 1 cycle sine waves with PGA amplitudes and equivalent 1 cycle sine wave period.

The spectra are shown in Figure 17 for the six representative records. Figures 17 and 5 are more similar than are Figures 12 and 5.

The averages of the difference ratios of all systems, $\bar{D}_P(P, R)$ given in Equation (7) for each input record, and their average for all records, $\bar{\bar{D}}_P(P)$, given in Equation (8), are shown in Table IV. The difference ratios of all the systems and records $\bar{\bar{D}}_P(P)$, using the equivalent 1 cycle sine wave period, T_e, are smaller than for any period investigated in Section 5, with no large difference ratios of all systems $\bar{D}_P(P, R)$ for any record.

The difference ratios $D_P(P, R, H, \mu_a, T)$ obtained with Equation (6), using T_e, are shown in Figure 13(d) for the six representative records when the hysteresis model is bilinear Takeda's ($\alpha = 0$) and the allowable ductility factor μ_a is 4. Compared to T_m, T_v, and T_p, the values are smaller on the whole, with no large difference ratios for any record.

Since the required strength can be obtained with 15 per cent average discrepancy using 1 cycle sine waves, strong ground motion can be simplified to a 1 cycle sine wave whose amplitude is the PGA and whose period is that of an equivalent 1 cycle sine wave calculated by the method described above.

Consequently, the required strength spectra, which express actual damage to structures (results of Section 3), are approximately determined by the PGA and the equivalent 1 cycle sine wave period. The 1 cycle sine wave periods, calculated from elastic response acceleration spectra, therefore can be used as the sole index to express frequency characteristics of strong ground motions. Although the mean period, T_m, can be used instead of the equivalent 1 cycle sine wave period, T_e, it is a little less accurate.

When predicting strong ground motions to be used in earthquake-resistant designs, only the relationship between the characteristics of the earthquake and site (the magnitude, inhomogeneity or directivity parameters in the case of near-field earthquakes, distance from the rupture plane, and ground surface properties) and the PGA and an equivalent 1 cycle sine wave period need to be examined. The relationship between earthquake characteristics and the mean period has been investigated [16] and the mean period was shown to be more closely related to the earthquake characteristics than the predominant period.

In our study, the acceleration amplitude and number of cycles of the sine waves were assumed to be constantly equal to PGA and 1 for simplicity. If these two factors are varied, smaller

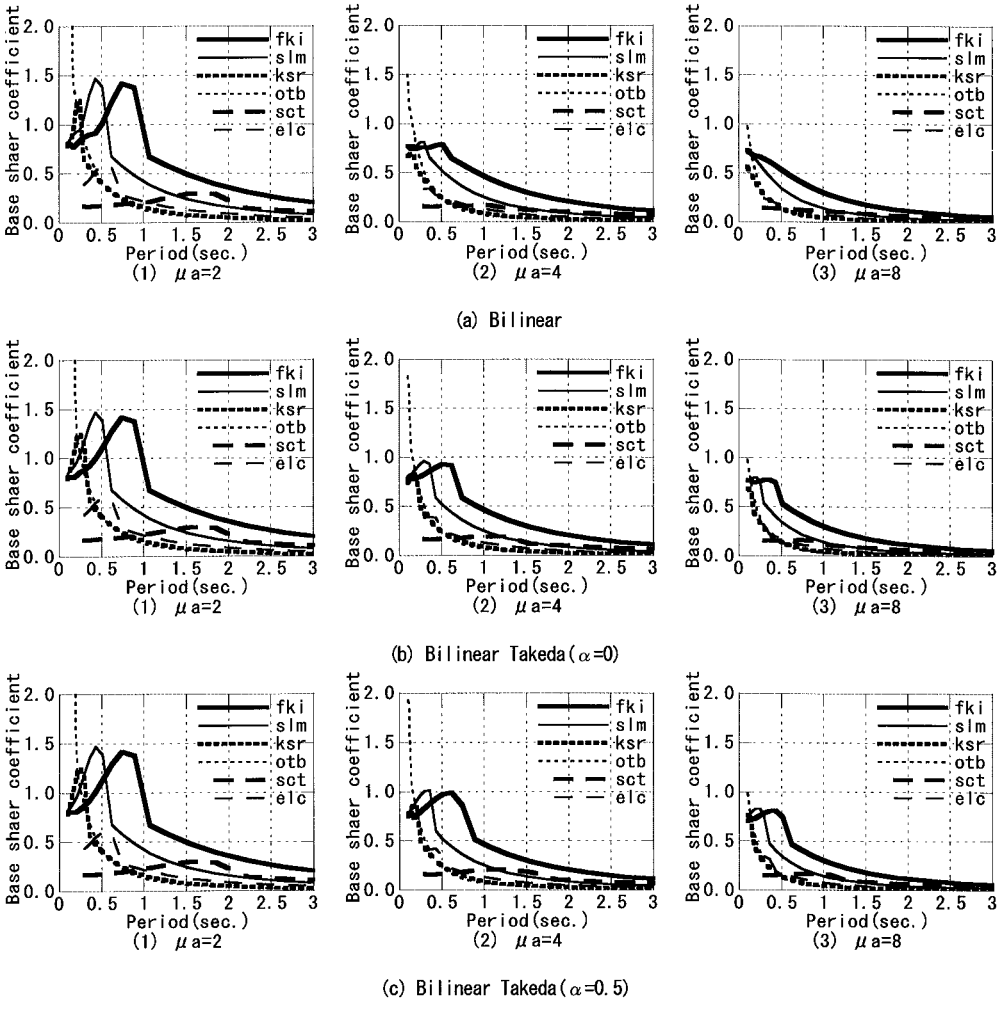

Figure 17. Required strength spectra from the equivalent 1 cycle sine waves.

discrepancy may result between the required strength spectra of the strong ground motions and sine waves.

7. CONCLUSION

Elastic and inelastic earthquake response analyses and response analyses under sine wave input using single-degree-of-freedom systems (SDOF systems) were made to investigate the simplification of strong ground motions to 1 cycle sine waves considering the inelastic seismic responses of structures.

First, the elastic and inelastic earthquake responses were analysed in order to calculate the required strength spectra which give maximum response ductility factors within 2, 4 and 8. A close relationship was shown between the spectra and actual structural damage.

Next, elastic and inelastic response analyses were made using sine waves. Only the acceleration amplitude and period of the sine waves need to be considered, neglecting the cycle number of the sine waves, if large plastic deformation with ductility factor more than 2 was assumed. This is because the approximate maximum responses of sine waves are determined by the first cycle due to the period elongation and plastic energy dissipation of the systems.

On the basis of the response analyses made with the input of sine waves, we made inelastic response analyses using 1 cycle sine waves whose acceleration amplitudes are the PGAs and whose periods are the predominant periods, as well as other periods of strong ground motions in order to calculate the required strength spectra. The required strength spectra from strong ground motions and 1 cycle sine waves were similar even for records with many cyclic reversals. In particular records, however, the discrepancy between the required strength spectra of the strong ground motions and 1 cycle sine waves was large. The period of the 1 cycle sine waves was then investigated in order to make the discrepancy small.

We proposed a method for simplifying strong ground motion to a 1 cycle sine wave whose acceleration amplitude is the PGA and whose period is that of an equivalent 1 cycle sine wave. The equivalent 1 cycle sine wave period is easily obtained from the elastic response acceleration spectra. The required strength can be evaluated with 15 per cent average discrepancy.

This means that the required strength spectra, which express the actual damage to structures, are approximately determined by the PGA and an equivalent 1 cycle sine wave period. The equivalent 1 cycle sine wave period therefore can be used as the sole index that expresses the frequency characteristics of strong ground motions.

Thus, when predicting strong ground motion to be used in earthquake-resistant designs, only the relationships between the characteristics of earthquake and site (the magnitude and inhomogeneity or directivity parameters in the case of near-field earthquakes, the distance from the rupture plane, and the ground surface properties) and PGA and an equivalent 1 cycle sine wave period need to be examined.

ACKNOWLEDGEMENTS

We thank the staff of Osaka Gas Company; JR Railway Technical Research Institute; Japan Meteorological Agency; Port and Harbor Research Institute, Ministry of Transport; and the Committee on Earthquake Observation and Research in the Kansai Area; the staff of the Strong Motion Data Base at the Institute for Crustal Studies, University of California, Santa Barbara; Prof. K. Kudo the Earthquake Research Institute, University of Tokyo, and Prof. T. Sasatani the University of Hokkaido all of whom provided strong ground motion records.

REFERENCES

1. Newmark NM, Hall WJ. *Earthquake Spectra and Design*. Earthquake Engineering Research Institute, 1982.
2. Watabe M, Ohashi Y, Hasebe H. Research on design earthquake ground motions for high-rise buildings (Part 1). *Summaries of Technical Papers of Annual Meeting, Architectural Institute of Japan, B Structures* 1985; **1**:135–136 (in Japanese).
3. Editorial committee for the report on the Hanshin-Awaji earthquake disaster. Report on the Hanshin-Awaji earthquake disaster, General Issues, vol. 2, 1998 (in Japanese).

4. Nakamura Y, Uehan F, Inoue H. Waveform and analysis of the 1995 Hyogo-Ken-Nanbu Earthquake II. *JR Earthquake Information* 1996; (23d) (in Japanese).
5. Sakai Y, Tasai A, Kumazawa F, Kashiwazaki T. Damage to buildings caused by the 1993 Kushiro-oki earthquake. *Bulletin of the Earthquake Research Institute*, *University of Tokyo* 1993; **63** (Part 3/4):243–291 (in Japanese).
6. Kudo K, Sasatani T, Effects of surface soil and earthquake source radiation on the ground motion of 1.6g acceleration, observed during the August 8, 1993, South-West off Hokkaido earthquake, Japan – preliminary analysis. *Proceedings of the International Workshop on Strong Motion Data*, Menlo Park, CA, 1993; **2**:361–376.
7. U.S. Department of Commerce, National Oceanic and Atmospheric Administration, San Fernando, California, Earthquake of February 9, 1971, 1973.
8. California Department of Conservation Division of Mines and Geology. The 1984 Morgan Hill, California earthquake, special publication 68, 1984.
9. California Department of Conservation Division of Mines and Geology. CDMG Strong-motion records from the Morgan Hill, California earthquake of 24 April 1984, *Office of strong motion Studies Report* OSMS 84-7, 1984.
10. California Strong Motion Instrumentation Program. Processed CSMIP Strong-motions records from the Northridge, California earthquake of January 17, 1994, Release No. 1, 1994.
11. Sakai Y, Minami Y, Nakano Y, Ohami K, Maeda M, Shiohara H, Damage to buildings caused by the 1994 Northridge earthquake and earthquake response analyses by recorded strong ground motions. *Bulletin of the Earthquake Research Institute*, *University of Tokyo* 1994; **69** (Part 4):351–378 (in Japanese).
12. Otani S. Hysteresis models of reinforced concrete for earthquake response analysis. *Journal of the Faculty of Engineering*, *The University of Tokyo* (*B*) 1981; **XXXVI**(2):407–441.
13. Takeda T, Sozen MA, Nielsen NN. Reinforced concrete response to simulated earthquakes. *Journal of Structural Division*, ASCE, 1970; **96**(ST12):2557–2573.
14. Architectural Institute of Japan. Data on buildings for earthquake-resistant design 1981 (in Japanese).
15. Sakamoto I. Relationship between natural periods and nonlinearity of wooden dwellings. *Summaries of Technical Papers of Annual Meeting*, *Architectural Institute of Japan*, *C Structures* 1986; **2**:1187–1188 (in Japanese).
16. Rathje EM, Abrahamson NA, Bray JD. Simplified frequency content estimates of earthquake ground motions. *Journal of Geotechnical and Geoenvironmental Engineering*, ASCE 1998; **124**(2):150–159.

